arXiv:astro-ph/0309188v1 5 Sep 2003

THE EVOLUTIONARY STATUS OF M3 RR LYRAE VARIABLES:
BREAKDOWN OF THE CANONICAL FRAMEWORK?

M. CATELAN
Pontificia Universidad Católica de Chile, Departamento de Astronomía y Astrofísica,
Av. Vicuña Mackenna 4860, 782-0436 Macul, Santiago, Chile; email: mcatelan@astro.puc.cl
ApJ, in press

ABSTRACT

In order to test the prevailing paradigm of horizontal-branch (HB) stellar evolution, we use the large databases of measured RR Lyrae parameters for the globular cluster M3 (NGC 5272) recently provided by Bakos et al. and Corwin & Carney. We compare the observed distribution of fundamentalized periods against the predictions of synthetic HBs. The observed distribution shows a sharp peak at $P_{\rm f} \approx 0.55$ d, which is primarily due to the RRab variables, whereas the model predictions instead indicate that the distribution should be more uniform in $P_{\rm f}$, with a buildup of variables with shorter periods ($P_{\rm f} < 0.5$ d). Detailed statistical tests show, for the first time, that the observed and predicted distributions are incompatible with one another at a high significance level. Either this indicates that canonical HB models are inappropriate, or that M3 is a pathological case that cannot be considered representative of the Oosterhoff type I (OoI) class. In this sense, we show that the OoI cluster with the next largest number of RR Lyrae variables, M5 (NGC 5904), presents a similar, though less dramatic, challenge to the models. We show that the sharp peak in the M3 period distribution receives a significant contribution from the Blazhko variables in the cluster. We also show that M15 (NGC 7078) and M68 (NGC 4590) show similar peaks in their $P_{\rm f}$ distributions, which in spite of being located at a similar $P_{\rm f}$ value as M3's, can however be primarily ascribed to the RRc variables. Again similar to M3, a demise of RRc variables towards the blue edge of the instability strip is also present in these two globulars. This is again in sharp contrast with the evolutionary scenario, which also foresees a strong buildup of RRc variables with short periods in OoII globulars. We speculate that, in OoI systems, RRab variables may somehow get "trapped" close to the transition line between RRab and RRc pulsators as they evolve to the blue in the H-R diagram, whereas in OoII systems it is the RRc variables that may get similarly "trapped" instead, as they evolve to the red, before changing their pulsation mode to RRab. Such a scenario is supported by the available CMDs and Bailey diagrams for M3, M15, and M68.

Subject headings: Galaxy: globular clusters: individual: M3 (NGC 5272), M5 (NGC 5904), M15 (NGC 7078), M53 (NGC 5024), M68 (NGC 4590) – stars: horizontal-branch – stars: variables: other

1. INTRODUCTION

For many years, M3 (NGC 5272) has been considered the canonical globular cluster (GC) par excellence. Lowly reddened, relatively nearby, and having a long history of detailed observations, M3 was early noted to contain hundreds of RR Lyrae (RRL) variables, making it a "splendid object for further studies" (Bailey 1902). This, of course, was confirmed by all subsequent analyses (Bakos, Benkö, & Jurcsik 2000; Corwin & Carney 2001; Clement et al. 2001 and references therein), which revealed that M3 is the GC with the largest (known) number of RRL variables, apart from ω Centauri (NGC 5139). Hence it is not surprising to find that M3 is the prototype of the so-called Oosterhoff type I (OoI) variability class (Oosterhoff 1939). For comparison purposes, the other OoI cluster noted by Oosterhoff, M5 (NGC 5904)—also the OoI GC with the second largest number of RRL variables—contains ~ 100 fewer known RRL variables than M3.

In the present paper, we take benefit of the uniquely large number of RRL variables in M3 to perform, for the first time, a detailed statistical comparison between the predictions of the standard model of horizontal-branch (HB) evolution and RRL pulsation and the observed periods. In particular, our aim is to investigate whether the discrepancy between predicted and observed period distributions originally noted by Rood & Crocker (1989) is confirmed by the current models. In §2, we describe our analysis techniques. In §3, we compare the RRL variables in the inner and outer regions of M3.

In §4, we describe our reference M3 models, which are then compared against the observations. In §6, we discuss the impact of different assumptions about the instability strip (IS) topology upon our results. Finally, in §7, we discuss possible explanations for the discrepancies we find, and extend our analysis to the cases of other GCs.

2. ANALYSIS

We retrieved and employed the catalogues of RRL periods, photometric properties and coordinates from Bakos et al. (2000)[1] and Corwin & Carney (2001). These contain a total of > 200 RRL with determined periods that can be used in our analysis. Info from these catalogues includes periods, variability type and mode of pulsation, information on the presence (or otherwise) of the Blazhko effect, colors, magnitudes, and radial distance from the center of the cluster. At the outset, we note that the mean period of the fundamental-mode pulsators (RRab's), $\langle P_{\rm ab} \rangle = 0.559 \pm 0.005$ d, as well as the number fraction of first-overtone pulsators (RRc's), $22 \pm 2\%$, confirm Oosterhoff's (1939) definition of the OoI group based on M3.

The simulations employed in the present paper are similar to those described in Catelan, Ferraro, & Rood (2001). In particular, the evolutionary tracks are the same as those computed by Catelan et al. (1998), and assume a main sequence chemical composition $Y_{\rm MS} = 0.23$, $Z = 0.001$; the HB stars have an

---

[1] http://www.konkoly.hu/staff/bakos/M3/table.html.

envelope helium abundance $Y_{HB} = 0.2409$, due to the extra helium brought to the surface during the first dredge-up. The HB synthesis code, SINTDELPHI, is an updated version of Catelan's (1993) code. To compute a synthetic HB, the code assumes that the mass distribution on the zero-age HB (ZAHB) is a normal deviate (Rood 1973; Caputo et al. 1987; Lee 1990; Catelan et al. 1998). This standard assumption is now known to break down in the cases of at least some of the so-called "bimodal HB clusters" (e.g., Rood et al. 1993; Catelan et al. 1998, 2002), as well as in clusters with significant populations of "extreme HB stars" (e.g., D'Cruz et al. 1996)—but has generally been considered a reasonable approximation for clusters with "well-behaved" HBs such as the ones we model in the present paper (e.g., Lee 1990), and even in clusters with long blue tails such as M79 (Dixon et al. 1996). Note, in addition, that the adoption of normal *deviates*, as opposed to strictly normal distributions, along with the fact that the HB synthesis technique adopts a Monte Carlo approach, implies that individual cases drawn from large pools of simulations will often bear little resemblance to an actual Gaussian distribution.

By default, the blue edge (BE) of the IS is computed for each individual star as a function of its basic physical parameters (L, M, Y_{HB}) using eq. (1) of Caputo et al. (1987), which is based on the Stellingwerf (1984) pulsation models. Then, for each star, the temperature of the red edge (RE) of the IS is obtained based on a free input parameter, the width of the IS $\Delta \log T_{eff}^{IS}$, that is supplied at run time. If the temperature of the star falls in between the so-computed blue and red edges of the IS, it is then flagged as an RRL variable, and its (fundamental) pulsation period computed according to eq. (4) in Caputo, Marconi, & Santolamazza (1998)—an updated version of the van Albada & Baker (1971) period-mean density relation. In §6, we will discuss the implications of alternative formulations for the IS edges upon our results.

In obtaining the "best-fitting" HB simulations, we start from the solutions provided by Catelan et al. (2001), in the case of M3 (see §§§4,5,6), and by Catelan (2000), in the case of M5 (see §7); the reader is referred to these papers for an assessment of the quality of the fits. In the present paper, whenever changes in the input parameters (mean mass on the ZAHB and mass dispersion) are required in comparison with those studies—due, for instance, to changes in the placement of the BE of the IS—we make sure, in particular, that these "perturbed" solutions, which in general differ only slightly from the original ones, also provide excellent matches to the observed number counts along the cluster HBs, i.e., $B, V, R/(B+V+R)$.

3. INNER VS. OUTER REGIONS

Given the recent discovery (Catelan et al. 2001; Catelan, Rood, & Ferraro 2002) that the HB morphology of M3 is significantly bluer in the innermost regions ($r < 50''$) than in the outermost ones ($r > 210''$), and predictions, based on stellar evolution theory and the period-mean density relation, that the pulsation periods of RRL stars may depend on the HB type (e.g., Lee, Demarque, & Zinn 1990), we have initially investigated whether the period distribution of RRL variables may differ between the two noted radial regions. In order to perform the test, we have followed the recommendations of van Albada & Baker (1973), "fundamentalizing" the RRc variables by adding 0.128 to the logarithm of their periods. We then ran a Student t-test to check whether the distributions of fundamentalized periods over the two noted radial

regions are different, finding instead a $\simeq 47\%$ probability that the two distributions are derived from the same parent distribution. This is confirmed by a two-sample Kolmogorov-Smirnov (K-S) test, which implies that the two distributions are drawn from the same parent distribution with 84.5% probability.

We thus conclude that the range in HB type within M3, though significant, is insufficient to affect the pulsation properties of its variables, so that it is safe to employ the complete sample of M3 variables in our tests. This conclusion is fully supported by HB simulations independently computed for the inner and outer regions of the cluster.

4. GLOBAL ANALYSIS

Extending thus the HB number counts reported in Catelan et al. (2001) over all radial regions of M3 (F. R. Ferraro 2000, priv. comm.), we obtain $B + V + R = 530$, $B : V : R = 0.39 : 0.40 : 0.21$, and $(B-R)/(B+V+R) = +0.183$. The best-fitting, canonical, unimodal HB simulation that best reproduces these parameters, under the prescription for the BE of the IS discussed in §2, and adopting for the width of the RRL strip the canonical value $\Delta \log T_{eff}^{IS} = 0.085$ (Smith 1995, §1.2.3 and Table 1.1), is characterized by a mean ZAHB mass value and a mass dispersion given by, respectively,

$$\langle M_{HB} \rangle = 0.641 \, M_\odot, \quad \sigma_M = 0.019 \, M_\odot. \quad \text{(Case A)}$$

Not surprisingly, both of these parameters are intermediate between the values for the "inner" and "outer" solutions given in Catelan et al. (2001). These are the parameters that we shall use in §5 ("Case A"). Cases B and C will be described in §6.

5. THEORY VERSUS OBSERVATIONS

We first compare the predicted and observed (fundamentalized) period distributions using a two-sample K-S test. A set of 5000 simulations with the input parameters described in §4 ("Case A") yields a mean probability that the computed and observed periods are drawn from the same parent distribution of $\langle P_{KS} \rangle \approx 4.5 \times 10^{-6}$. The highest value of P_{KS}, in these simulations, was 0.29%. Thus, the simulated and observed period distributions are different at a high significance level. Following Rood & Crocker (1989), we attribute this to the peaked shape of the M3 distribution, which is shown in Fig. 1, left panel, along with the co-added, normalized simulations. We have checked that the comparison between models and observations, as shown in Fig. 1, remains qualitatively unchanged when the number of bins is allowed to vary in the range from 15 to 25, with the bin size automatically computed from the number of bins and the plot limits 0.25 d and 1.05 d. Note that our statistical analysis is *insensitive* to the binning, since it relies on a K-S test; the histograms are shown only for illustration purposes, and to highlight the period ranges over which the discrepancy between models and observations is most severe (see §6 for a more detailed discussion).

In order to further test the frequency of "peaked" period distributions that might resemble M3's, we have also computed the standard deviation of the fundamentalized period distribution for all the simulations. This could be relevant, in particular, if peaked distributions occurred somewhat randomly in P_f space, the precise location of the M3 peak not bearing particular significance. We find $\langle \sigma_{P_f} \rangle = 0.116 \pm 0.006$ d (standard deviation), whereas the observed value is $\sigma_{P_f} = 0.077$ d. Thus the observed distribution is intrinsically more "peaky" than the simulated ones—a 6σ result. Clearly, Case A simulations cannot provide a good description of M3 RRL properties.
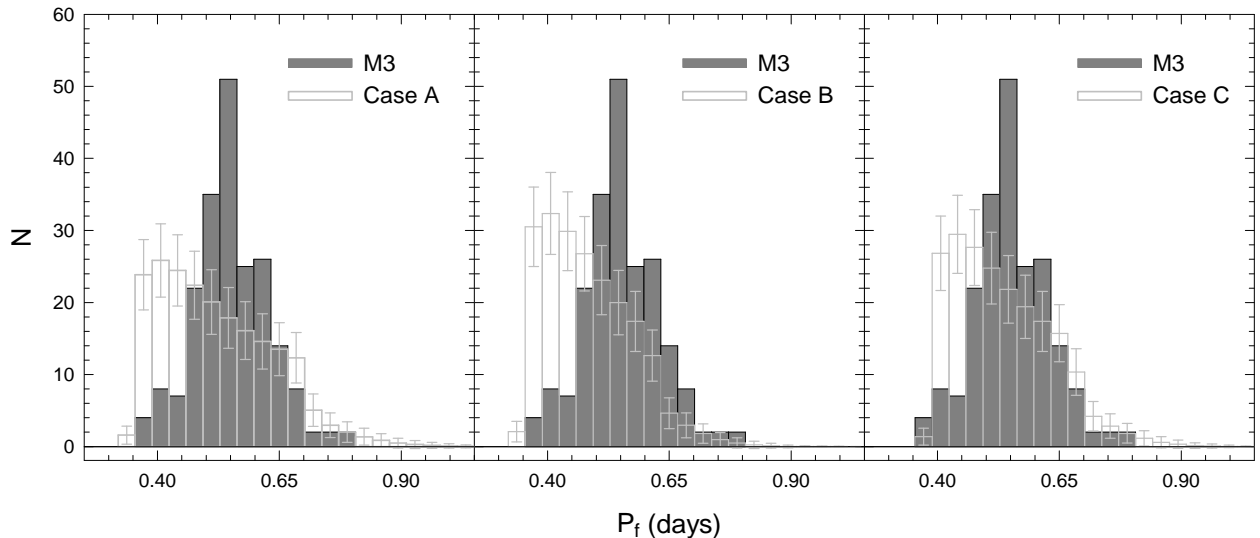
FIG. 1.— Histogram of fundamentalized periods of M3 RRL variables: Observations: filled bars; normalized simulations: light gray bars, with Poissonian errors indicated.

We provide the histograms for three simulations computed in this way in the top row of Fig. 2 ("Case A"), where the models with the largest P_{KS} and smallest σ_{P_f} are given in the left and middle panels, respectively. The right panel in that row corresponds to a randomly picked simulation from the remaining pool of 4998 synthetic HBs. Note that the axis scales and bin sizes are identical to the ones used in Fig. 1.

Analysis of these plots discloses that the theoretical models, besides presenting much less sharp peaks than observed, also present a build-up of stars at short periods which is not matched by the observed distribution. This is due to the fact that the RRc side of the IS is as well populated as the RRab side, as can be seen by the H-R diagram and $\log T_{\mathrm{eff}}$ histogram for the co-added Case A simulations (Fig. 3, bottom right and top panels), and also to the fact that relatively fainter regions of the H-R diagram tend to be more populated (due to slower evolution) than the brighter parts of the IS at a given temperature (Fig. 3, bottom panels). The signature of these brighter stars can be identified in the long-period "tail" that is seen in the theoretical period histograms; however, the drop from the peak to this long-period tail is more abrupt in the data, which is also reflected upon the systematically smaller observed σ_{P_f} in comparison with the predicted values. Note that qualitatively similar features had previously been found by Rood & Crocker (1989), whose results are fully supported by our simulations.

We call attention, in passing, to the fact that the ZAHB strictly corresponds to a lower, fairly thinly populated lower envelope to the distribution in the H-R diagram (Fig. 3), the bulk of the HB stars being found at slightly larger luminosities, while the HB stars are evolving on blue loops. Such a phenomenon was obvious in previous studies as well—see, e.g., Fig. 4b in Catelan (1993), Fig. 17 in Catelan et al. (1998), and also Ferraro et al. (1999). For this reason, it appears unlikely to us that the stars that tend to clump around the "OoI line" in the Bailey diagram are actual "ZAHB stars," as suggested by Clement & Hazen (1999). We suggest instead that many of these stars are more likely to be "blue loop stars." Also in passing, we note that the RRL which have been found "below the ZAHB" in M3 (Corwin & Carney 2001; see also

Jurcsik 2003) may simply be a consequence of an imperfect analogy between zero-age MS, on the one hand—a line very close to which low-mass MS stars will indeed spend most of their MS lifetimes—and ZAHB, on the other—the ZAHB *not* being, in general, a line very close to which RRL/HB stars will spend most of their HB lifetimes.

6. INSTABILITY STRIP EDGES

The results of Catelan et al. (2001) indicate that the IS boundaries, calculated as described in §2, provide a good description of the M3 IS boundaries (see Fig. 1 in Catelan et al.). The color transformations adopted in Catelan et al. correspond to an earlier version of the VandenBerg & Clem (2003) transformations, which were kindly provided by D. A. VandenBerg (1999, priv. comm.) prior to publication. Note that the (average) temperature of the BE of the IS, as computed in §5 following the prescriptions described in §2, is ≈ 7420 K, thus being similar to the canonical value reported in Smith (1995).

However, Smith (1995) also cautions that such a BE may be too hot, "perhaps by 100–200 K"—and current pulsation models do seem to favor a slighly cooler BE for the relevant metallicities ($Z \approx 0.001 - 0.002$), as can be seen from Table 1 in Caputo et al. (2000; see also Bono et al. 1997). It is interesting to note that the quoted Caputo et al. pulsation models, for parameters similar to those implied by our simulations for the M3 RRL variables—namely, mean mass $\langle M_{\mathrm{RR}} \rangle \simeq 0.645\,M_\odot$, mean luminosity $\langle \log(L_{\mathrm{RR}}/L_\odot) \rangle \simeq 1.67$—imply an IS width that is even larger than what we assumed in §5, namely, $\Delta \log T_{\mathrm{eff}}^{\mathrm{IS}} = 0.086 - 0.089$. The BE of the IS is found, according to these models, at about $T_{\mathrm{eff}} \simeq 7150 - 7250$ K; this is consistent with Smith's remark about a possible shift of the IS towards lower temperatures. Moreover, it appears reasonable to assume that the RE of the IS—hence the IS width, once the BE temperature is fixed—remains more uncertain than the BE at the present time, in spite of the efforts that were made in the quoted papers to take into account nonlocal and time-dependent convective effects in the nonlinear computations (see also Feuchtinger 1999)—ingredients which, along with the choice of mixing-length parameter, do not play as significant a role in the case of the IS BE. Moreover, the conversion
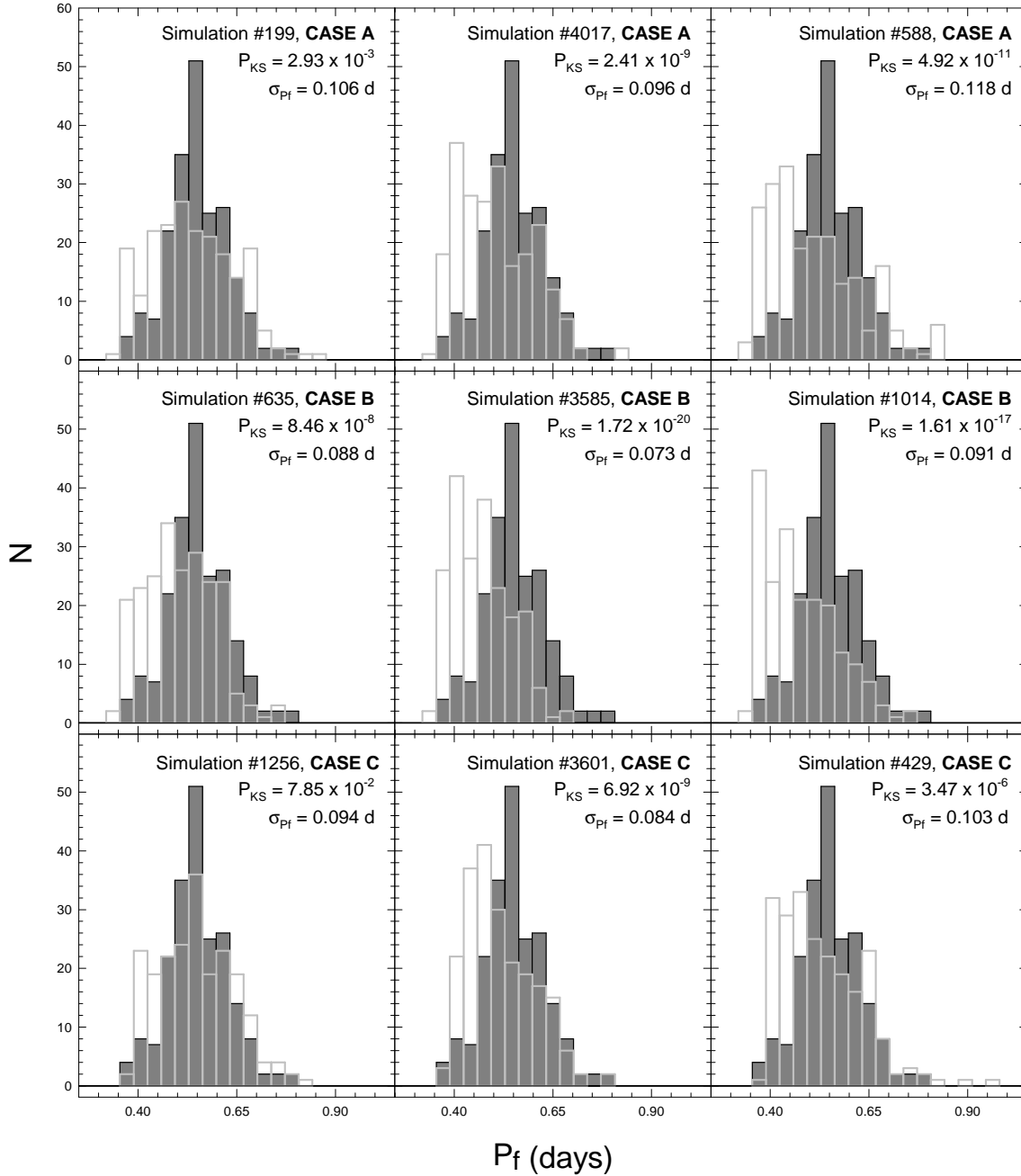
FIG. 2.— Period distributions for synthetic HB models for M3 (light gray bars), compared with the observations (filled bars). Top row: "Case A" models, which assume an IS width of $\Delta \log T_{\rm eff}^{\rm IS} = 0.085$ and have a blue edge of the IS at $T_{\rm eff} \simeq 7400$ K. Middle row: "Case B" models, which are similar to Case A models but assume a narrower IS width, $\Delta \log T_{\rm eff}^{\rm IS} = 0.070$. Bottom row: "Case C" models, which assume the same IS width as in Case B, but whose blue edge of the IS is cooler by 200 K. For each case, we have, from left to right: the model with the highest $P_{\rm KS}$; the model with the smallest $\sigma_{P_{\rm f}}$; and a randomly picked model.

between colors and temperatures is still not without uncertainties at the RRL level—see, e.g, the comparison among predictions by different authors in Figs. 3, 4, and 19 of VandenBerg & Clem (2003), bearing in mind the possible suggested ranges in RRL temperatures, from ~ 5800 K (Caputo et al. 2000, their Table 1) to ~ 7400 K (Smith 1995). For these reasons, at the present time, we cannot rule out the possibility that the IS is significantly narrower than we have assumed thus far. In fact, Fig. 7 in Popielski, Dziembowski, & Cassisi (2000), which seems to be based on a combination of theoretical models for the BE and empirical results for the RE, supports an IS width, at the luminosity level of the RRL in our simulations,

of $\Delta \log T_{\rm eff}^{\rm IS} \simeq 0.079$, the width decreasing with decreasing luminosity.

Therefore, in order to investigate the impact of IS topology uncertainties upon our results, we have also computed extensive sets of HB simulations for the following additional situations: "Case B" has an IS width reduced to $\Delta \log T_{\rm eff}^{\rm IS} = 0.070$; "Case C" not only has a narrower strip, but also a BE shifted by -200 K.[2] For these cases, we now find that the best-fitting

[2] The referee notes that a new preprint has recently come out (Marconi et al. 2003) in which pulsation models are reported according to which the IS BE is indeed 226 ± 66 K cooler than in our Case A models.
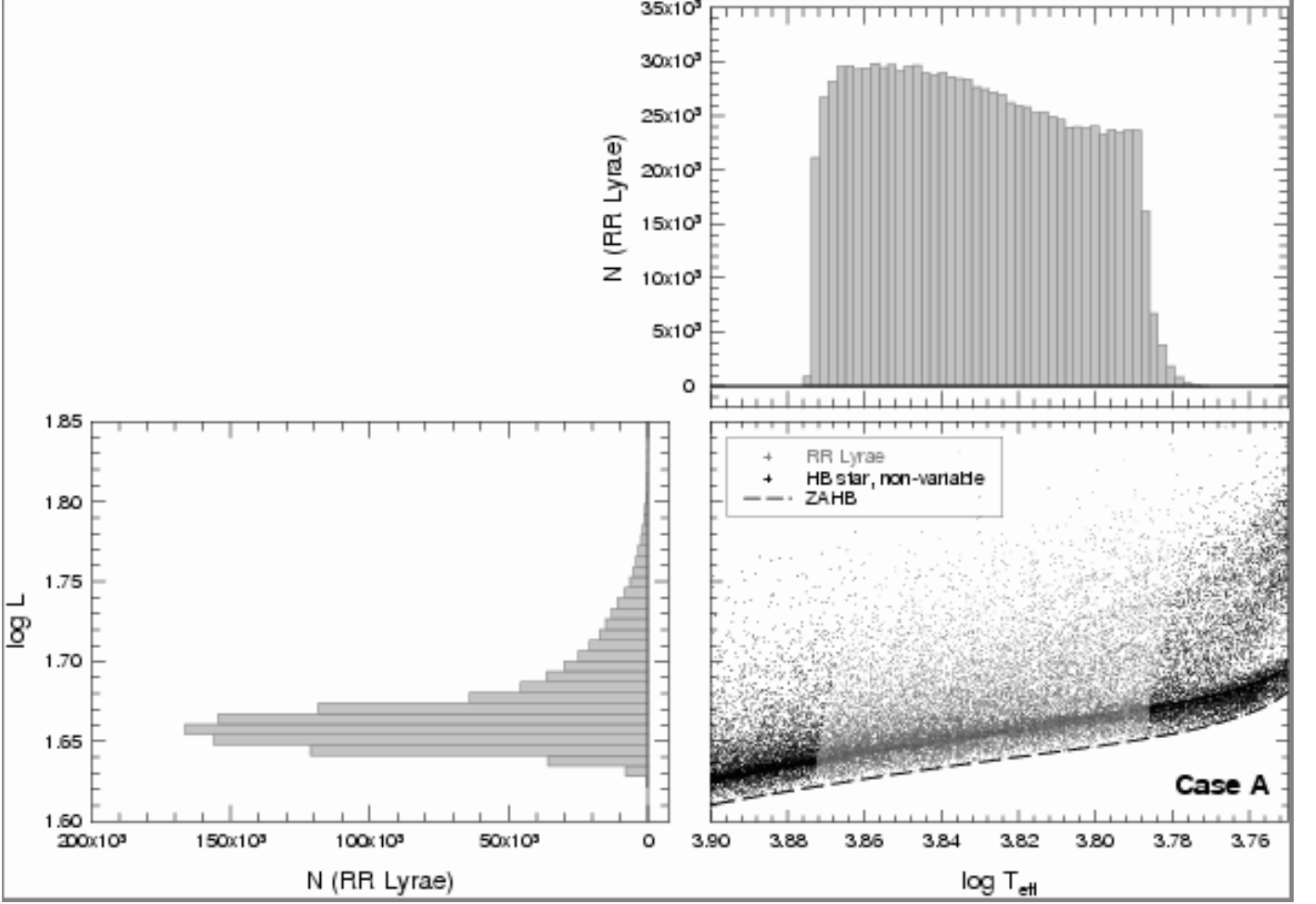
FIG. 3.— The H-R diagram at the bottom right, centered around the RRL region, represents a subsample of 20,000 RRL stars from the complete pool of 1,076,042 RRL stars in the 5000 simulations for Case A. A proportional number of non-variable HB stars is also shown. The temperature and luminosity histograms (top and left panels, respectively) refer to the full set of RRL stars from the Case A simulations. In the H-R diagram, the ZAHB line is indicated. Note the fairly uniform temperature distribution, and the sharply peaked luminosity distribution at a luminosity level well *above* the ZAHB.

HB simulations are described by the following input parameters:

$$\langle M_{\rm HB} \rangle = 0.640\,M_\odot, \quad \sigma_M = 0.015\,M_\odot; \qquad \text{(Case B)}$$

$$\langle M_{\rm HB} \rangle = 0.643\,M_\odot, \quad \sigma_M = 0.015\,M_\odot. \qquad \text{(Case C)}$$

These are fairly similar to the Case A solution for the mean ZAHB mass and mass dispersion (§4), differences only appearing in the third decimal place for both quantities. However, the implications upon the predicted period distributions are more immediately apparent.

Thus, for Case B, we find $\langle P_{\rm KS} \rangle \approx 4.4 \times 10^{-11}$, with the highest $P_{\rm KS}$ in the 5000 simulations being 8.5×10^{-8}. Clearly, the discrepancy is even more significant in this case. We interpret this as being due to the necessity of producing synthetic HBs that match the observed number of RRL variables in M3: if the IS width is reduced, one must redistribute the variables that formerly fell on the low-temperature, longer-period end of the distribution to the other regions of the IS. Given that the highest probability for an RRL variable is to fall in the shorter-period, "pile-up" region (which is not seen in the data), that region is enhanced even further in this case, leading to an exacerbation of the problem. These effects are shown very clearly in the middle panel of Fig. 1. On the other

hand, this case also gives a smaller $\langle \sigma_{P_{\rm f}} \rangle = 0.090 \pm 0.005$ d, which however is still inconsistent with the observed $\sigma_{P_{\rm f}}$ at the 2.7σ level. The cases with the largest $P_{\rm KS}$ and smallest $\sigma_{P_{\rm f}}$, besides a randomly selected one, are given in the left, middle, and right panels, respectively, of the middle row of Fig. 2. We emphasize that, while some of these simulations do present reasonably sharp peaks, those peaks are invariably at the short-period end of the distribution, unlike the case in M3. Hence we conclude that Case B simulations do not provide a good description of the M3 period distribution either.

Finally, Case C provides $\langle P_{\rm KS} \rangle \simeq 7.21 \times 10^{-4}$ and $\langle \sigma_{P_{\rm f}} \rangle = 0.100 \pm 0.005$ d. The highest $P_{\rm KS}$ found in the 5000 simulations for this case is 7.9%. Therefore, Case C represents an improvement over the previous ones, though it is still far from being able to provide a satisfactory match to the observed distribution. The improvement chiefly results from the fact that, by moving the IS BE to a lower temperature, we are effectively "forcing" some of the RRL stars out of the "pile-up region" at the short-period end of the distribution—a feature which we have seen not to be present in the data. The flipside of the coin is that this also feeds the longer-period end of the distribution with more variables, resulting in a higher value of $\langle \sigma_{P_{\rm f}} \rangle$—in this case, inconsistent with the observed $\sigma_{P_{\rm f}}$ at the 4.4σ level. In those simulations where the period distribu-
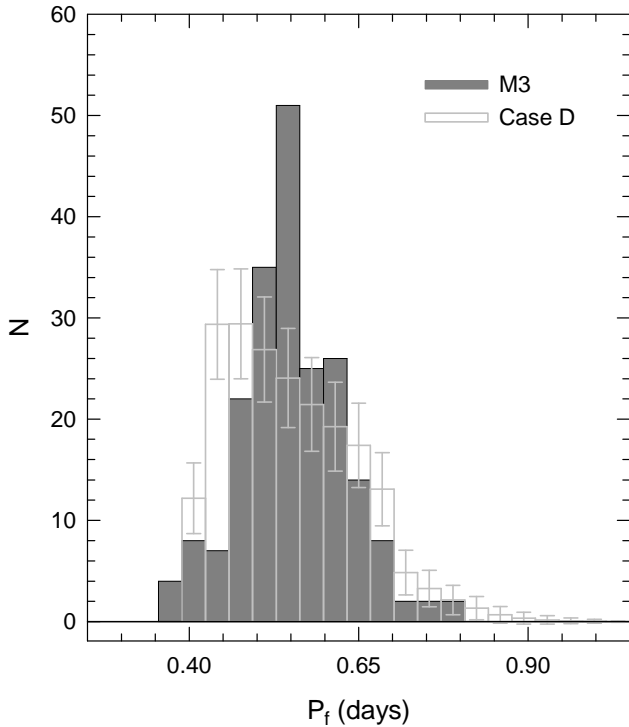
FIG. 4.— As in Fig. 1, but assuming a $\Delta \log T_{\mathrm{eff}}^{\mathrm{IS}} = 0.065$, and shifting the BE by -300 K with respect to Case A.

tion does turn out to be peaky, such as in the middle panel in the bottom row of Fig. 2, the peak is still located towards the short-period end of the distribution, unlike the observed one which is primarily due to the RRab stars. Hence Case C simulations cannot be considered satisfactory at explaining the shape of the M3 distribution.

Based on these results, one might wonder whether shifting the BE of the IS to even lower temperatures in order to further deplete the short-period end of the distribution, while at the same time decreasing the IS width even further in order to avoid an exacerbation of the discrepancy between predicted and observed $\sigma_{P_{\mathrm{f}}}$ values, could not bring about an additional improvement in the situation. To test this possibility, we have pushed both the BE temperature and IS width to what might arguably be their lowest possible bounds, computing thus a set of 5000 simulations for a BE that is cooler than in Case A by 300 K, and an IS width $\Delta \log T_{\mathrm{eff}}^{\mathrm{IS}} = 0.065$. We will refer to this rather extreme combination as "Case D" in what follows.

The co-added Case D simulations are compared against the M3 distribution in Fig. 4. One now finds that the short-period end of the distribution has been somewhat depleted, the minimum period been noticeably longer than had been found heretofore. However, there still remains a predicted excess of short-period stars with periods $P_{\mathrm{f}} \lesssim 0.45$ d, as well as an excess of longer-period RRL with periods $P_{\mathrm{f}} \gtrsim 0.65$ d.

As a consequence of the smaller number of short-period stars, the statistical tests for Case D do reveal some improvement with respect to the previous cases. The corresponding figures for this new case are as follows: $\langle P_{\mathrm{KS}} \rangle \simeq 2.3\%$ (with a maximum $P_{\mathrm{KS}} = 42.4\%$) and $\langle \sigma_{P_{\mathrm{f}}} \rangle = 0.097 \pm 0.005$ d. However, one should note that still only 4.7% of the Case D simulations are found with $P_{\mathrm{KS}} > 10\%$. Moreover, the computed $\langle \sigma_{P_{\mathrm{f}}} \rangle$ value is still inconsistent with the observed one, at the 4σ level; in terms of Fig. 4, this is clearly indicated by the

remaining excess of both short- and longer-period RRL stars compared to the observations. Hence, in spite of a rather extreme combination of IS width and placement which should have minimized the discrepancy between models and observations, Case D is also unable to satisfactorily account for the M3 period distribution.

Is it possible that the noted discrepancy could be traced to the specific set of evolutionary tracks employed? In order to test this possibility, we have also computed HB simulations following a procedure similar to that described in §§2-5, but using instead the evolutionary tracks computed by Castellani, Chieffi, & Pulone (1991). We again computed sets of 5000 HB simulations for each of Cases A, B, and C. We find that the results depend but slightly on the actual set of HB tracks employed. For Case A, we find $\langle P_{\mathrm{KS}} \rangle \approx 1.7 \times 10^{-4}$, with a highest value of $P_{\mathrm{KS}} \simeq 7.6\%$; for Case B, we find $\langle P_{\mathrm{KS}} \rangle \approx 2.5 \times 10^{-9}$, with a highest value of $P_{\mathrm{KS}} \simeq 1.1 \times 10^{-6}$; finally, for Case C we obtain $\langle P_{\mathrm{KS}} \rangle \approx 0.66\%$, with a highest value of $P_{\mathrm{KS}} \simeq 17.9\%$ (but only about 0.5% of all simulations presenting $P_{\mathrm{KS}} \geq 10\%$). The standard deviations of the computed period distributions are very similar to the values obtained using the original set of evolutionary tracks, being only slightly larger. The co-added, normalized simulations for these three cases are shown in Fig. 5, which should be directly compared against Fig. 1. It is clear that the histograms for the same cases considered in Fig. 1 and Fig. 5 are very similar, only careful scrutiny revealing some small differences, particularly in the size of the build-up towards short periods. Clearly, the contrast between models and observations, first noted by Rood & Crocker (1989), cannot be simply due to the specific set of HB models adopted in the simulations, though further experiments using different sets of evolutionary tracks might also prove instructive.

In addition, one might wonder whether, if the RRL luminosities predicted by our models are incorrect, eventual changes in the HB luminosity might not lead to better agreement between the predicted and observed period distributions. In this sense, the histograms in Fig. 1 indicate that a major problem with the canonical predictions is that they foresee too many short-period variables, compared to the observations. Given the well-known fact that the RRL IS is sloped in the H-R diagram, with the blue and red edges becoming cooler as the luminosity increases, a higher predicted luminosity for the RRL would move the IS BE towards lower temperatures, thus decreasing the number of expected short-period variables and increasing the number of expected longer-period RRL.

The mean absolute magnitude of the RRL in our simulations, at $Z = 0.001$, is around $M_V = 0.615$ mag. Assuming, for M3, the amount of alpha-enhancement provided in Table 2 of Carney (1996), and using the prescriptions of Salaris, Chieffi, & Straniero (1993), this corresponds to a $[\mathrm{Fe/H}] = -1.49$. Given the available calibrations of the HB absolute magnitude, is there much room for an increase in the HB luminosity over our value?

We can take a representative calibration of the "long" (i.e., bright) RRL distance scale (Walker 1992), and evaluate what HB magnitude should be expected for the quoted $[\mathrm{Fe/H}]$ value. According to Walker's eq. (3), we get $M_V = 0.507$ mag at $[\mathrm{Fe/H}] = -1.49$. Hence our predicted HB is fainter than foreseen by "bright" calibrations of the HB luminosity by 0.108 mag, or by 0.043 in $\log L$. Given the dependence of the slope of the IS BE on luminosity from several different sources (e.g., Popielski et al. 2000; Caputo et al. 1987), we find that this has but a small impact on the temperature of the
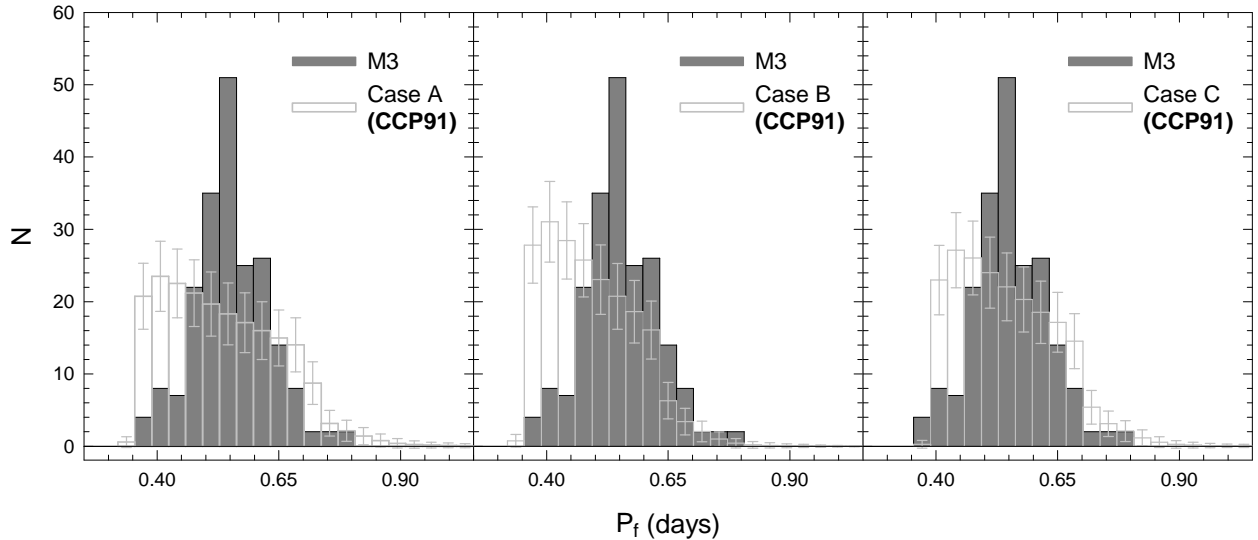
FIG. 5.— As in Fig. 1, but with simulations computed using the Castellani et al. (1991, CCP91) evolutionary tracks. Note that the results are very similar to those shown in Fig. 1.

BE, with $\delta \log T_{\mathrm{eff}}^{\mathrm{BE}} < 0.0035$. This, according to the period-mean density relation, implies a shift in the minimum periods towards longer values by $\delta \log P \lesssim +0.012$, or a shift from the "pile-up" values in Fig. 1 from $P \approx 0.38$ d to $P \lesssim 0.391$ d. This will readily be seen as too little to explain the discrepancy between model predictions and the observations in regard to the existence and placement of the pile-up at short periods. On the other hand, one may also note that if the luminosity shift is simultaneously taken into account, one finds instead a shift of the pile-up period to $P \lesssim 0.425$ d. However, the luminosity effect operates on the whole of the IS, so that the conflict between models and observations that is apparent at the longer-period end of the distributions in Fig. 1 would become even more pronounced, especially for Cases A and C. For Case B, the change would effectively be similar to the one previously carried out when going from Case B to Case C. We conclude that the only way for a change in predicted HB luminosity to help explain the observations would be for the IS to get even narrower than 0.07 as the luminosity increased. However, according to Fig. 7 in Popielski et al. (2000), the IS width actually *increases* with increasing HB luminosity.

Note that usage of pulsation periods in these tests renders us immune to the intrinsic problems related to the determination of equilibrium colors and temperatures of RRL stars (Rood & Crocker 1989; Bono, Caputo, & Stellingwerf 1995).

7. BREAKDOWN OF THE CANONICAL FRAMEWORK?

M3's peaked period distribution was already obvious in Oosterhoff's (1939) Fig. 1, and also in Fig. 36 of Christy (1966), Fig. 2 of Stobie (1971), Fig. 23 of Cacciari & Renzini (1976), Fig. 5b of Castellani & Quarta (1987), and Fig. 7 of Corwin & Carney (2001). Rood & Crocker (1989) were the first to note that this distribution might be in conflict with the models, though no statistical tests were performed at the time. More than a century after Bailey's (1902) data were collected, and some 64 years since Oosterhoff used such data to produce a plot first showing the sharp peak in the M3 period distribution, we are now able, for the first time, to establish that the M3 period distribution is incompatible with canonical model predictions.

What is the reason for the discrepancy? This is unclear at present, but R. T. Rood (2003, priv. comm.) has hypothesized that slower evolution, possibly related to pulsationally-induced mass loss (Willson & Bowen 1984), close to the transition region between RRab and RRc pulsators, could "trap" stars there and lead to the observed feature. Indeed, a connection between RRL pulsation (which is traditionally thought of as an "envelope-only" phenomenon) and interior evolution has previously been made in regard to period change rates (e.g., Sweigart & Renzini 1979; Rathbun & Smith 1997), but also in terms of a possible connection between mass loss, HB evolution, and the RRd phenomenon (Koopmann et al. 1994). While it is not clear how exactly the aforementioned effect might operate in the case of OoI GCs, the following might be a possibility for OoII GCs, which seem to present a similar pile-up effect among its RRc stars (see below). One might conjecture that the redward-evolving RRL, when reaching the c-ab transition line, might suffer a sudden episode of mass loss, which might be sufficient to momentarily drive *blue-ward* evolution for the star (Koopmann et al. 1994). However, as soon as the star evolved away from the transition line, mass loss would cease, and the evolution would then proceed along a similar redward path as was originally the case—until the transition line is reached again. While the connection with pulsation is speculative, a similar kind of "evolutionary trapping" related to mass loss was indeed found in the detailed evolutionary computations by Koopmann and co-authors. Further calculations similar to those carried out by Koopmann et al. would certainly prove worthwhile. It might also be interesting to study the role of rotation in this regard, particularly given its suggested connection with the Blazhko effect (see, e.g., Smith et al. 2003 and references therein)—which, as we shall see, may also contribute to the pile-up effect in M3.

Inspection of the M3 CMD at the RRL region (Bakos & Jurcsik 2000; Corwin & Carney 2001) does reveal that the ab region is much more densely populated than the RRc region. This is in sharp contrast with the canonical model predictions, in which the RRL strip is fairly uniformly populated from blue to red (Fig. 3), and the larger number of RRab variables compared to the RRc ones in OoI globulars is primarily due to
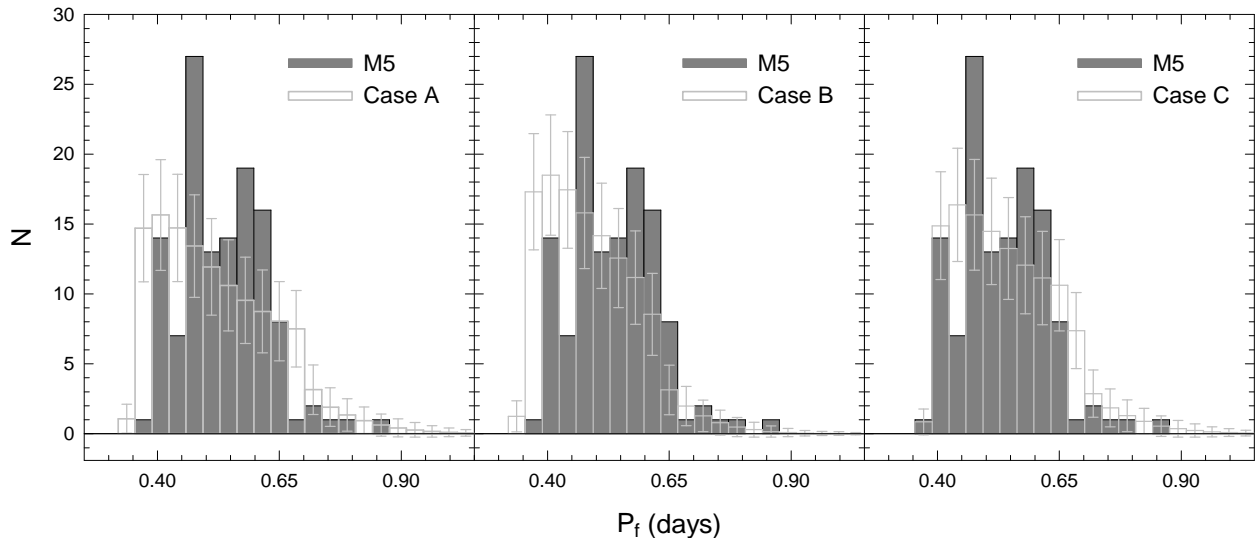
FIG. 6.— As in Fig. 1, but for M5.

evolutionary hysteresis (van Albada & Baker 1973), not to a "pile-up" of stars in the RRab region (see, e.g., Fig. 3 in Caputo, Castellani, & Tornambè 1978). In this regard, it is worth noting that the hysteresis mechanism implies a large overlap in temperatures and colors between RRab and RRc pulsators (Catelan 1993), which is *not* observed in M3 (Bakos & Jurcsik 2000; Corwin & Carney 2001).

In order to provide an ad-hoc explanation for the color distribution of M3 RRL's within the scope of standard evolutionary models, we would be forced to invoke a multimodal mass distribution on the ZAHB (Rood & Crocker 1989). One possibility that immediately comes to mind is to invoke one sharply peaked mass mode lying inside the RRab region, another primarily responsible for the blue HB and RRc components, and a third one accounting for the bulk of the red HB stars. However, it is unlikely that such an ad-hoc solution would prove satisfactory, given the fact that HB evolutionary tracks for the relevant metallicity show pronounced "blue loops" away from the ZAHB: if all stars started their HB evolution at the same ZAHB location, a significant spread in temperatures (hence periods) should still be expected, as is particularly evident from Fig. 3 in Caputo et al. (1978) and Figs. 6b and 9b from Catelan et al. (2001).

Given the presence of these blue loops, one might then speculate that the ZAHB mass distribution peak responsible for the observed pile-up should actually be placed just to the red side of the IS, wherefrom a blue loop just long enough to reach the pile-up region would originate. According to our models, and assuming hysteresis operates in the "either-or" zone, such a loop corresponds to a ZAHB mass of about $0.655 M_\odot$ (with a ZAHB position $\log T_{\rm eff} \simeq 3.789$). In this scenario, another ZAHB mass peak would be located farther to the red along the red HB, and a third one on the blue HB. In this case, the demise of short-period RRc stars would be explained by the fact that i) the region of the BE of the IS would correspond to the tail of this mass mode; ii) the blue HB stars would not spend enough time inside the RRL strip as they evolve redward to the asymptotic giant branch. The one problem with this ad-hoc explanation is that it fails to explain the existence of sharp peaks in the period distributions of OoII GCs as well, as we will see below, at least under the canonical framework—which invokes redward evolution for the RRL stars, and most certainly also red HB stars, in OoII globulars.

Another effect which may be of importance in interpreting Fig. 1 is provided by Fig. 1 in Bakos & Jurcsik (2000), which suggests that the RRab variables presenting the Blazhko effect are more clumped in M_V than their non-Blazhko counterparts. We confirm that the Blazhko RRab's do have narrower M_V, color, and period distributions, compared to the non-Blazhko RRab variables. The corresponding standard deviations of the distributions, for the non-Blazhko RRab's, are $\sigma_V = 0.085$ mag, $\sigma_{B-V} = 0.034$ mag, $\sigma_{P_{\rm f}} = 0.064$ d; whereas for the Blazhko variables we find instead $\sigma_V = 0.069$ mag, $\sigma_{B-V} = 0.030$ mag, $\sigma_{P_{\rm f}} = 0.049$ d. However, we caution that, in spite of the consistently smaller standard deviations in the Blazhko case, two-sample K-S tests are not able to confirm that the Blazhko and non-Blazhko RRL have significantly different distributions in any of these parameters. Therefore, the suggested difference should be subject to further tests before it can be considered real.

Is the peaked distribution in fundamentalized periods a universal characteristic of OoI systems, or does it instead reveal a problem that somehow applies exclusively to M3? Fig. 1 in Oosterhoff (1939) already suggested that the M5 period distribution is flatter than M3's—thus indicating that the latter's sharply peaked distribution is likely not due to the existence of a very numerous, but yet undetected, population of low-amplitude RRL stars. In Fig. 6 we provide a histogram of fundamentalized periods for the RRL variables in M5, similar to what was done in Fig. 1 for M3. The plot is based on data provided in the Clement et al. (2001) online catalogue, and implies a $\sigma_{P_{\rm f}} = 0.088$ d. This is indeed larger than the value derived for M3, which is consistent with our interpretation that M3's small $\sigma_{P_{\rm f}}$ is due in part to a relatively unpopulated RRc region: the fraction of RRc stars is higher in M5 than in M3, with approximately 30% of the M5 RRL's pulsating in the first overtone mode.

Are models specifically computed for M5 able to reproduce its period distribution? To investigate this, we have computed additional sets of 5000 HB simulations with input parameters similar to those described for M5 in Catelan (2000), and
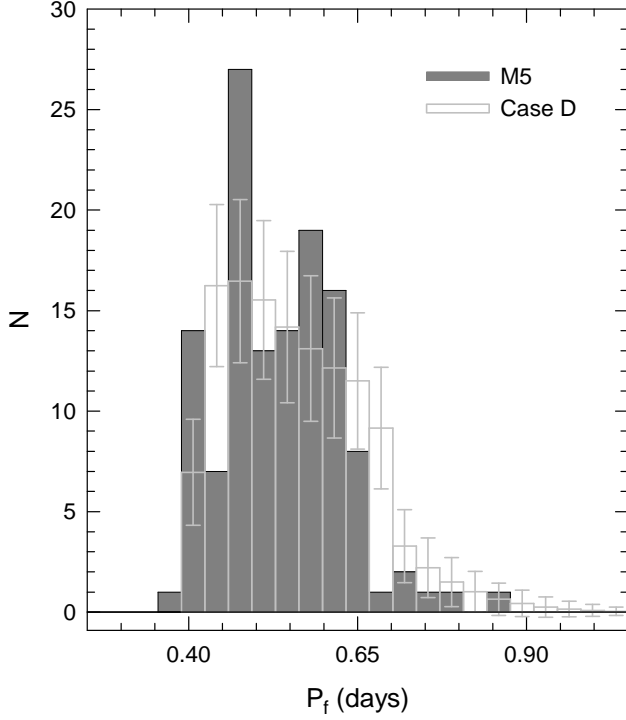
FIG. 7.— As in Fig. 4, but for M5. The statistics reveals this case to be less successful than Case C at reproducing the M5 period distribution, contrary to what happens in the case of M3.

analogous to Cases A, B, C for M3 (§§5,6). Those were compared with the observed period distribution using a two-sample K-S test. For Case A, we find a mean probability of $\approx 5\%$ that the observed and computed distributions are drawn from the same parent distribution. The models also give $\langle \sigma_{P_f} \rangle = 0.121 \pm 0.008$ d—which is inconsistent with the observed value at the 4.3σ level. Case B models for M5, in turn, give $\langle P_{KS} \rangle \approx 5.6 \times 10^{-3}$ and $\langle \sigma_{P_f} \rangle = 0.094 \pm 0.007$ d. As for M3, the K-S test shows worse agreement between models and observations for a smaller IS width, although the smaller computed σ_{P_f} is now consistent with the observed one. Finally, Case C models for M5 yield $\langle P_{KS} \rangle \approx 27\%$ and $\langle \sigma_{P_f} \rangle = 0.106 \pm 0.008$ d. While the standard deviation differs from the observed value at the 2.2σ level, the K-S test now indicates that some satisfactory matches between models and observations can be achieved for M5 in this case, with the maximum P_{KS} found in the Case C simulations being 98.7% and 15.7% of them being found with $P_{KS} \geq 50\%$. Detailed comparisons between models and observations for M5 are presented in Fig. 6. We note, in addition, that while the Case D simulations improved the agreement between observed and predicted period distributions somewhat in the case of M3, the same does not happen in the case of M5, for which the agreement deteriorates instead: for Case D, we find $\langle P_{KS} \rangle \approx 12.1\%$ (with a maximum $P_{KS} = 76.9\%$, but only 0.66% of the simulations being found with $P_{KS} \geq 50\%$), and $\langle \sigma_{P_f} \rangle = 0.103 \pm 0.008$ d. Comparison between the 5000 co-added Case D simulations and the M5 observations is provided in Fig. 7.

The somewhat better agreement between models and observations, in the case of M5, is due to the presence of a more substantial population of short-period RRc variables in this cluster compared to M3 (in spite of a substantially larger overall RRL population in the latter), along with a less pronounced

peak in the M5 period distribution. Additional studies of the M5 RRL population based on the image-subtraction package ISIS (Alard 2000) might prove very important in defining the relative proportion of short-period, low-amplitude RRc's (and RRab's) in this cluster, and in conclusively establishing whether pronounced peaks in the RRL period distribution similar to M3's might be present in this cluster as well. In this sense, it should also be extremely important to establish whether the population of Blazhko variables in M5 is indeed a mere two or three stars, as currently indicated by the Clement et al. (2001) catalogue, because the peaked period distribution in M3, as we have seen, seems to receive a significant contribution from the Blazhko variables that are present in that cluster.

We can also check to see whether the noted anomaly is a characteristic solely of OoI systems, or whether instead it also affects OoII globulars. In Fig. 8, we show the fundamentalized period distributions for RRL variables in the three OoII GCs with the largest number of RRL according to the Clement et al. (2001) catalogue, namely: M15 (NGC 7078), M53 (NGC 5024), and M68 (NGC 4590). The period values were taken directly from the Clement et al. entries; in the case of M68, we adopted the entries corresponding to the Walker (1994) study. Due to the smaller number of variables in OoII GCs, a smaller number of bins was used in this case, though again we find our results, qualitatively, to be insensitive to the specific choice of bin number and size. As in the cases of M3 and M5 previously discussed, we have fundamentalized the periods of the RRc's by adding 0.128 to their log-periods. A similar procedure was applied to any double-mode (RRd) or (candidate) second-overtone (RRe) pulsator that might be present. Note that the fraction of RRd plus RRe variables, compared to the total numbers of RRc, RRd, and RRe pulsators, is small in M53 (6.7%) and M15 (14.5%), but not so in M68 (43%). These fractions are even smaller in the cases of M3 and M5; in the latter, there is not a single RRd variable according to the Clement et al. catalogue, and but one RRe candidate; whereas in the former, it appears that fewer than 4% of the RRL are RRd or (candidate) RRe pulsators.

Unfortunately, detailed statistical tests are not as conclusive in the case of OoII GCs, given the intrinsically smaller number of RRL compared to the case of M3, or even M5. Moreover, it has been argued in the literature that, whereas there are indications that the RRL variables in OoII systems are indeed evolved away from a position on the blue ZAHB, canonical models fail to produce such evolved RRL in adequate numbers (Pritzl et al. 2002 and references therein). Therefore, until the evolutionary status of the RRL in OoII GCs is adequately established, a detailed statistical comparison between the predictions of canonical HB models and the observed period distributions in OoII GCs may not prove conclusive. For this reason, we defer such a detailed comparison between models and observations for OoII GCs to a future occasion.

Qualitatively though, one may note, from Fig. 8, that at least M15 and M68 do show signs of having a sharp peak in their period distributions, whereas the same is not as obvious in the case of M53, in spite of its larger number of RRL variables (compared to M68). Interestingly, the peak in the period distribution is located at a similar (perhaps slightly shorter) period in comparison with the case of M3. Moreover, there is again no sign of a pile-up at the shorter periods, even though the pile-up effect might perhaps be expected to be strong in OoII globulars as well, if RRL variables are evolved away
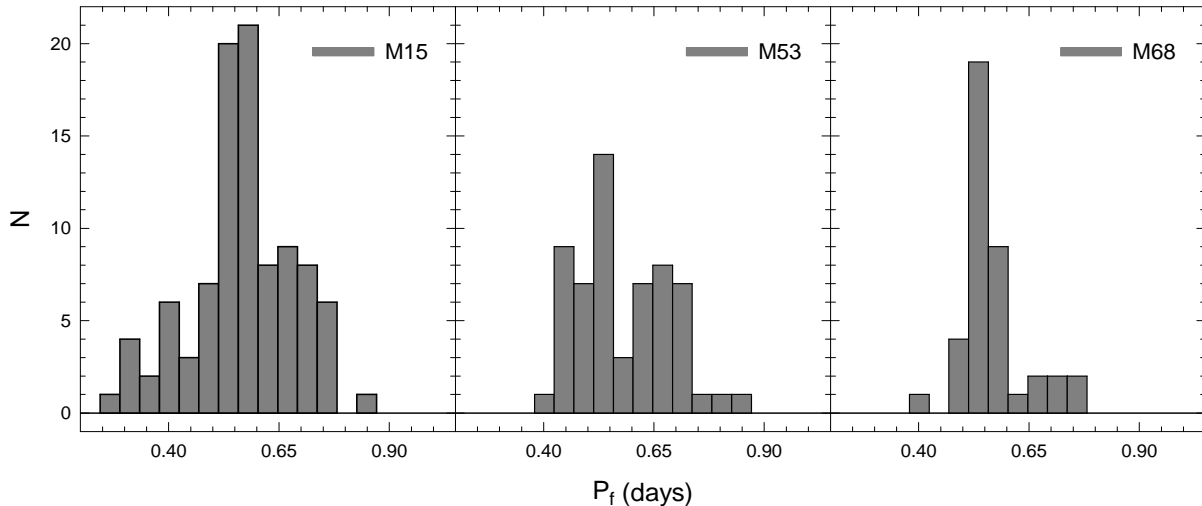
Fig. 8.— Fundamentalized period distributions for the RRL in well-populated OoII GCs: M15 (left), M53 (center), and M68 (right).

from a position on the blue ZAHB, since in this case (redward) evolution would be slower close to the BE of the IS than close to the IS RE (Catelan 1994; see also Figs. 3d,e in Caputo et al. 1978). The standard deviations of the period distributions, in the cases of M15 and M53—$\sigma_{P_f} = 0.117$ d and 0.107 d, respectively—are consistently larger than found previously for M3 and M5. On the other hand, the M68 distribution, with $\sigma_{P_f} = 0.074$ d, seems even narrower than is the case for the OoI GCs.

In the spirit of Rood's speculative scenario for the pile-up of stars on the RRab side of the IS in OoI systems, one may hypothesize that the same is happening in at least some OoII GCs, but *on the opposite side of the IS*—that is, on the RRc side. Hence, in OoI systems, the RRL might get "trapped" just to the red of the RRab-RRc transition line, while they are evolving blueward; whereas, in OoII systems, the RRL might instead get "trapped" just to the blue of this transition line, in the course of their redward evolution. If so, we would expect to find evidence, in OoII GC CMDs and Bailey diagrams, of a pile-up of RRc variables close to the transition line.

In this regard, we first note that the peaks in the M15 and M68 period distributions are indeed primarily due to the RRc variables; the case of M68 is particularly noteworthy. This cluster has 15 RRc stars, 14 of which have periods in the range 0.34 to 0.39 d, corresponding to fundamentalized periods 0.47 to 0.52 d. The single exception is V5, with a period of 0.282 d. Perhaps not surprisingly, we do find most of these RRc's located close to the transition line between RRc and RRab variables—see, for example, Fig. 13 in Walker (1994). In the case of M15, the lack of a CCD study of its variables based on state-of-the-art photometric data obtained under good seeing conditions limits our current possibilities; however, interesting indications are already provided by the Bingham et al. (1984) photographic study, as well as by the V, R data obtained by Silbermann & Smith (1995). In the CMD showing the detailed topology of the IS from Bingham et al. (see their Fig. 14), one again encounters a clear pile-up of the RRc variables close to the c-ab transition line. That these stars are primarily responsible for the peak in the period distribution is particularly evident by confronting the quoted figure with Fig. 18 in the same paper; it is also seen that the RRd's contribute to the effect as well, being situated just to

the red (long-period side) of the peak in the period distribution. Importantly, one again finds a demise of RRc variables close to the BE of the IS, contrary to what is predicted by the simulations: it is difficult to see, in the canonical evolutionary scenario, how the middle region of the IS could be more heavily populated than the vicinity of the IS BE. These conclusions are also consistent with the Silbermann & Smith CMD (their Fig. 11), Bailey (Fig. 13), and period-color diagrams (Fig. 14). To the best of our knowledge, similar diagrams are currently lacking for M53.

Perhaps noteworthy as well is the suggested presence, in M15 and M53 alike (but not in M68), of a secondary "hump" in the period distributions, at around $P_f \approx 0.67$ d; a similar feature can be noted to be present in the cases of M3 and M5, though at a slightly shorter period—namely, $P_f \approx 0.62$ d. Such a feature is not generally present in the computed model distributions (see the co-added, normalized results in Figs. 1 through 7). Along with the lack of substantial populations of short-period RRc variables located close to the BE of the IS in the clusters that we have studied—which may actually constitute a fairly universal feature, judging from the plots in Cacciari & Renzini (1976) and Castellani & Quarta (1987), M5 possibly representing an exception to this rule—besides the sharp period distributions in many of them, this seems to point to a serious challenge to our current understanding of the interplay between pulsation and evolution of RRL stars in GCs, and thereby of the Oosterhoff dichotomy itself. The yellow flag raised by Rood & Crocker back in 1989 is now looking quite red indeed.

REFERENCES

Alard, C. 2000, A&AS, 144, 363

Bailey, S. I. 1902, Annals of the Astronomical Observatory of Harvard College, Vol. XXXVIII

Bakos, G. Á., Benkö, J. M., & Jurcsik, J. 2000, AcA, 50, 221

Bakos, G. Á., & Jurcsik, J. 2000, in ASP Conf. Ser. 203, The Impact of Large-Scale Surveys on Pulsating Star Research, ed. L. Szabados & D. W. Kurtz (San Francisco: ASP), 255

Bingham, E. A., Cacciari, C., Dickens, R. J., & Fusi Pecci, F. 1984, MNRAS, 209, 765

Bono, G., Caputo, F., Castellani, V., & Marconi, M. 1997, A&AS, 121, 327

Bono, G., Caputo, F., & Stellingwerf, R. F. 1995, ApJS, 99, 263

Cacciari, C., & Renzini, A. 1976, A&AS, 25, 303

Caputo, F., Castellani, V., & Tornambè, A. 1978, A&A, 67, 107

Caputo, F., Castellani, V., Marconi, M., & Ripepi, V. 2000, MNRAS, 316, 819

Caputo, F., De Stefanis, P., Paez, E., & Quarta, M. L. 1987, A&AS, 68, 119

Caputo, F., Marconi, M., & Santolamazza, P. 1998, MNRAS, 293, 364

Carney, B. W. 1996, PASP, 108, 900

Castellani, V., Chieffi, A., & Pulone, L. 1991, ApJS, 76, 911

Castellani, V., & Quarta, M. L. 1987, A&AS, 71, 1

Catelan, M. 1993, A&AS, 98, 547

Catelan, M. 1994, A&A, 285, 469

Catelan, M. 2000, ApJ, 531, 826

Catelan, M., Borissova, J., Ferraro, F. R., Corwin, T. M., Smith, H. A., & Kurtev, R. 2002, AJ, 124, 364

Catelan, M., Borissova, J., Sweigart, A. V., & Spassova, N. 1998, ApJ, 494, 265

Catelan, M., Ferraro, F. R., & Rood, R. T. 2001, ApJ, 560, 970

Catelan, M., Rood, R. T., & Ferraro, F. R. 2002, in Extragalactic Star Clusters, IAU Symp. Series, Vol. 207, eds. D. Geisler, E. K. Grebel, & D. Minniti (San Francisco: ASP), 113

Christy, R. F. 1966, ApJ, 144, 108

Clement, C. M., et al. 2001, AJ, 122, 2587

Clement, C. M., & Shelton, I. 1999, ApJ, 515, L85

Corwin, T. M., & Carney, B. W. 2001, AJ, 122, 3183

D'Cruz, N. L., Dorman, B., Rood, R. T., & O'Connell, R. W. 1996, ApJ, 466, 359

Dixon, W. V. D., Davidsen, A. F., Dorman, B., & Ferguson, H. C. 1996, AJ, 111, 1936

Ferraro, F. R., Messineo, M., Fusi Pecci, F., De Palo, M. A., Straniero, O., Chieffi, A., & Limongi, M. 1999, AJ, 118, 1738

Feuchtinger, M. U. 1999, A&A, 351, 103

Jurcsik, J. 2003, A&A, 403, 587

Koopmann, R. A., Lee, Y.-W., Demarque, P., & Howard, J. M. 1994, ApJ, 423, 380

Lee, Y.-W. 1990, ApJ, 363, 159

Lee, Y.-W., Demarque, P., & Zinn, R. 1990, ApJ, 350, 155

Marconi, M., Caputo, F., Di Criscienzo, M., & Castellani, M. 2003, ApJ, in press (astro-ph/0306356)

Oosterhoff, P. Th. 1939, The Observatory, 62, 104

Popielski, B. L., Dziembowski, W. A., & Cassisi, S. 2000, AcA, 50, 491

Pritzl, B. J., Smith, H. A., Catelan, M., & Sweigart, A. V. 2002, AJ, 124, 949

Rathbun, P. G., & Smith, H. A. 1997, PASP, 109, 1128

Rood, R. T. 1973, ApJ, 184, 815

Rood, R. T., & Crocker, D. A. 1989, in IAU Colloq. 111, The Use of Pulsating Stars in Fundamental Problems of Astronomy, ed. E. G. Schmidt (Cambridge University Press, Cambridge), 218

Rood, R. T., Crocker, D. A., Fusi Pecci, F., Ferraro, F. R., Clementini, G., & Buonanno, R. 1993, in ASP Conf. Ser. 48, The Globular Cluster-Galaxy Connection, ed. G. H. Smith & J. P. Brodie (San Francisco: ASP), 218

Salaris, M., Chieffi, A., & Straniero, O. 1993, ApJ, 414, 580

Silbermann, N. A., & Smith, H. A. 1995, AJ, 110, 704

Smith, H. A. 1995, RR Lyrae Stars. Cambridge University Press, Cambridge

Smith, H. A., et al. 2003, PASP, 115, 43

Stellingwerf, R. F. 1984, ApJ, 277, 322

Stobie, R. S. 1971, ApJ, 168, 381

Sweigart, A. V., & Renzini, A. 1979, A&A, 71, 66

van Albada, T. S., & Baker, N. 1971, ApJ, 169, 311

van Albada, T. S., & Baker, N. 1973, ApJ, 185, 477

VandenBerg, D. A., & Clem, J. L. 2003, AJ, 126, 778

Walker, A. R. 1992, ApJ, 390, L81

Walker, A. R. 1994, AJ, 108, 555

Willson, L. A., & Bowen, G. H. 1984, Nature, 312, 429